Effect of increasing organic loading rates on the performance of moving-bed biofilm reactors filled with different support media: Assessing the activity of suspended and attached biomass fractions

J.P. Bassin*, I.N. Dias, S.M.S. Cao, E. Senra, Y. Laranjeira, M. Dezotti

Federal University of Rio de Janeiro, COPPE—Chemical Engineering Program, PO Box 68502, 21941-972 Rio de Janeiro, Brazil

ARTICLE INFO

ABSTRACT

In this study, two moving-bed biofilm reactors ($MBBR_1$ and $MBBR_2$) filled with different carrier media (Kaldnes K1 and Mutag Biochip, respectively) were subjected to increasing organic loading rates for 700 days. Regardless of the carrier used, both systems could withstand high organic loads up to $3.2\,kgCOD/(m^3\,d)$, condition under which complete ammonium removal was achieved. However, the type of media influenced the quantity and distribution of attached biomass in the support, which in turn affected the activity of specific microbial functional groups in the biofilm. As the chemical oxygen demand (COD) input was gradually increased, the biofilm got thicker and the surface detachment rates were enhanced. Consequently, the amount of suspended solids has increased considerably to levels commonly found in hybrid bioreactors. Activity batch tests have shown that the contribution of the bulk phase biomass to the overall nitrification was very significant, being more relevant as the biofilm sloughing events became more intense. At constant organic loading rate, the hydraulic retention time (HRT) had a noticeable impact on the nitrification process, as it directly influenced the fraction of ammonium oxidized either by the attached or suspended biomass. Total nitrogen removal amounted up to 86 and 73% in $MBBR_1$ and $MBBR_2$, respectively.

1. Introduction

In recent years, the stricter effluent quality requirements posed by environmental regulations around the world have pushed the development of space- and cost-effective wastewater treatment technologies with high performance. In this scenario, biofilm processes have increasingly drawn the attention of environmental engineers and researchers (Henze et al., 2008). The use of attached instead of suspended biomass allows for the construction of very compact reactors and provides an easier separation of the biosolids from the treated effluent. Moreover, in contrast to flocculent sludge technologies, the retention of biomass in attached growth processes is improved and can be controlled independently of the prevailing hydraulic conditions (Lewandowski and Beyenal, 2014). This particular feature is especially beneficial for the establishment and development of slow growing organisms which frequently suffer from washout as a result of hydraulic and

---

* Corresponding author. Tel.: +55 21 25628347; fax: +55 21 25628300.
  E-mail address: jbassin@peq.coppe.ufrj.br (J.P. Bassin).

organic shock loadings (Hu et al., 2011) and/or insufficient solids retention time (Head and Oleszkiewicz, 2005).

The moving-bed biofilm reactor (MBBR) is a growing biofilm technology which has gained much attention in the wastewater treatment sector in the last 20 years (Barwal and Chaudhary, 2014). It is based on the use of freely moving plastic carrier elements with density a little lighter than that of water in which microorganisms form biofilms (Ødegaard, 2006). Given the advantages shown by the MBBR process such as compactness, flexibility and high quality effluent production, a rapidly growing market for this technology has been established worldwide. In this context, many different types of commercial media have been developed for specific applications (van Haandel and van der Lubbe, 2012) and this biofilm process has been extensively used for the treatment of synthetic (Bassin et al., 2012a; Hoang et al., 2014), domestic (Bassin et al., 2011; Calderón et al., 2012) and industrial wastewaters (Bassin et al., 2011; Dvořák et al., 2014).

Part of the applications of the MBBR technology is focused on the treatment of high organic load waste streams, as investigated previously (Rusten et al., 1998; Melin et al., 2005; Aygun et al., 2008; Javid et al., 2013). Under such conditions, the development of fast-growing heterotrophs which outcompete nitrifying bacteria for oxygen and space in biofilm systems is favoured (Figueroa and Silverstein, 1992), whereas nitrification functionality may be hindered. Thus, investigating how nitrification behaves in MBBR systems subjected to high COD input is important to predict their overall treatment performance. Furthermore, as the carrier material employed in MBBR processes has been reported to influence the attachment and distribution characteristics of the biofilm (Chu et al., 2014), it is interesting to understand how the type of support media will affect the activity of nitrifiers in situations where overgrowth of heterotrophs takes place. Such information may potentially be used in the selection of suitable biofilm carriers for MBBRs treating high loaded wastewaters. So far, studies addressing the impact of the carrier material on the operation of MBBR have been restricted to low to medium organic load applications (Chu and Wang, 2011a,b; Chu et al., 2014).

MBBR systems are often characterized by low suspended solids content (Barwal and Chaudhary, 2014). Hence, their design and operation is usually based on surface loading rates, which are intrinsically dependent on the activity of the media-attached biomass (Ødegaard et al., 2000). On the other hand, the suspended biomass activity is usually neglected. However, depending on the hydraulic and organic load conditions, the amount of solids in the bulk phase arising from either biofilm detachment or growth in suspension can be significant (Kwok et al., 1998). This exchange of biomass between the liquid and solid media phases underlines the need of taking into consideration both the suspended and attached biomass fractions in the design and modelling of biofilm systems (Boltz et al., 2009; Mašic and Eberl, 2014). Recently, Piculell et al. (2014) conducted a comprehensive study addressing the removal of organic matter in MBBRs subjected to varying operational conditions. This particular work provided insightful findings regarding the heterotrophic activity of free-growing and attached biomass fractions and their contribution to the overall COD removal under different hydraulic retention times (Piculell et al., 2014). However, information on the nitrifying activity of suspended and attached biomass in MBBR systems subjected to increasing organic loads is poorly addressed in literature. Given that nitrification in biofilm systems is highly influenced by the

organic matter input (Figueroa and Silverstein, 1992), evaluating the activity of nitrifiers in the bulk and biofilm phases at different organic loading rates is important to understand how nitrifying bacteria respond to load variations and predict nitrification performance under different COD/N ratios.

In the light of this background, this work attempts to evaluate the impact of increasing organic loading rates on COD and nitrogen conversions in two lab-scale MBBRs operated on a long-term basis (700 days). In order to observe the influence of the support media on the overall treatment performance as well as on the dynamics of suspended and adhered biomass throughout the experiment, each reactor was filled with a particular type of biomass-supporting carrier differing in size, structure and shape. The distribution of the biofilm grown in the different media was characterized by image analysis whereas the nitrifying activity of the different biomass fractions and their relative importance to the overall nitrification process were monitored at all experimental conditions.

2. Material and methods

2.1. Operational conditions of the MBBR systems

The experiments were conducted in two lab-scale MBBR systems (MBBR$_1$ and MBBR$_2$) with a volume of 1 L, which were run in a continuous mode for 700 days. Throughout this study, the reactors were subjected to six different experimental conditions, presented in Table 1. The volumetric organic loading rate was gradually increased from runs 1–4. Subsequently (runs 4–6), both the influent COD and the HRT were proportionally decreased in order to keep the organic loading rate constant. This procedure was conducted to evaluate the effect of the HRT on the dynamics of attached and suspended biomass fractions and their corresponding nitrifying activities. Both reactors were inoculated with 100 mL of activated sludge from a municipal wastewater treatment plant (CEDAE—Alegria, Rio de Janeiro, Brazil) designed for COD removal and nitrification. To ensure controlled substrate concentrations, laboratory prepared wastewater was used as influent for the MBBRs. Sodium acetate (NaAc) and ammonium chloride (NH$_4$Cl) were used as organic carbon and nitrogen source, respectively. The influent synthetic medium (modified from Bassin et al., 2012b) was prepared with demineralized water and had the following composition: 1028.4 g/L NaAc·3H$_2$O (for influent COD of 400 mg/L), 382.14 mg/L NH$_4$Cl (for influent ammonium of 100 mgN/L), 55.5 mg/L KH$_2$PO$_4$ (12 mgP/L), 53 mg/L MgSO$_4$, 222.5 mg/L NaCl, and 589.3 mg/L NaHCO$_3$. Depending on the experimental condition, the medium composition was varied in order to obtain the desired influent COD and ammonium-nitrogen concentrations. Alkalinity (supplied as NaHCO$_3$) and phosphorus source (provided as KH$_2$PO$_4$) were also correspondingly dosed according to the bacterial nutrition requirements in each experimental stage. A trace elements solution whose composition was described previously (Bassin et al., 2012a) was added in a proportion of 0.5 mL/L of medium. The influent wastewater was stored under refrigeration (4 °C) at a pH of 7.5–8.0 until being fed to the reactors. To evaluate the effect of different types of support media on the treatment process, MBBR$_1$ was filled with Kaldnes® K1 carriers whereas MBBR$_2$ was filled with Mutag Biochip™ media (see Fig. S1, Supplementary material). These two carriers present a specific surface area for biomass adhesion of 500 and 3000 m^2/m^3, respectively. Further information about the characteristics of the support materials can

Table 1 – Operational conditions of the MBBR systems.							
Run	Influent COD (mg/L)	Influent ammonium (mgN/L)	HRT (h)	Volumetric organic loading rate (kgCOD/(m^3 d))	Surface organic loading rate (gCOD/(m^2 d))	Volumetric nitrogen loading rate (kgNH$_4^+$–N/(m^3 d))	Surface organic loading rate (gNH$_4^+$–N/(m^2 d))	Time of operation (days)
1	400	100	12	0.8	3.2	0.2	0.8	112[a]
2	800	100	12	1.6	6.4	0.2	0.8	112
3	1200	100	12	2.4	9.6	0.2	0.8	142
4	1600	100	12	3.2	12.8	0.2	0.8	134
5	800	100	6	3.2	12.8	0.4	1.6	100
6	400	50	3	3.2	12.8	0.4	1.6	103

[a] The first experimental run comprised a start-up phase for biofilm development, which lasted 20 and 30 days in MBBR$_1$ and MBBR$_2$, respectively.

be found in Table S1. In order to have the same surface area for biofilm development in both reactors, the filling fraction, i.e., the amount of support per volume of reactor ($V_{support}/V_{reactor}$) was chosen to be 50% and 8.3% for the MBBR$_1$ and MBBR$_2$, respectively. Hence, the specific surface area corresponded to 250 m^2/m^3. Taking into account the volume of the reactors (1 L), the total area available for establishment of the biofilm was 0.25 m^2. Air was introduced to the reactors through porous diffusers, placed at the bottom of each tank. The air flow was kept constant at around 4 L/min in order to have the same hydraulic conditions in all experimental runs. The distribution of air bubbles allowed to keep the carriers in suspension and provided satisfactory oxygen transfer into the bulk liquid. The dissolved oxygen (DO) concentration varied within the range of 4–5 mg/L. Ambient temperature was around 22 ± 4 °C and pH was maintained between 6.8 and 7.5 by adding either 1 M NaOH or 1 M HCl.

2.2. Additional experiments for assessment of nitrifying activity

In order to determine the maximum specific nitrifying activity of both attached and suspended biomass and estimate the amount of ammonium oxidized by each biomass fraction in the different experimental runs, two types of batch tests were conducted from runs 2 to 6. In this set of trials, the reactor feeding was stopped and a pulse of a concentrated stock solution of ammonium chloride was added in the beginning of the test in order to achieve initial ammonium concentrations similar to that of the reactor influent, i.e., 100 mgN/L. Samples were collected every 15 to 30 min for 6 h (360 min) for determination of the ammonium concentration. The volumetric ammonium removal rate was calculated by linear regression of ammonium concentration over time whereas the biomass-specific ammonium removal rate was determined by dividing the volumetric ammonium removal rate by the total amount of biomass (i.e., volatile total solids (VTS) = volatile attached (VAS) + suspended (VSS) solids) in the corresponding reactor. The approach used to discriminate between the amount of ammonium nitrified by the attached and suspended biomass was a bit different. Given the fact that this information cannot be assessed under normal operating conditions as both attached and suspended solids are present within the systems, it was decided to remove one of the biomass fractions. Hence, it was opted to remove all the plastic carriers from the two reactors and therefore keep only the suspended biomass. Otherwise, if the test was performed only with the supports by removing the suspended solids, detachment of biomass from the carriers would eventually occur over the experiment

and therefore the conversions would not be only attributed to the biofilm but also to the bulk phase biomass activity. Similarly to the previous experiment, the volumetric ammonium removal rate obtained with each type of biomass fraction was estimated by linear regression of the ammonium concentration over time. The contribution of suspended biomass to the overall ammonium removal, expressed in percentage, was estimated by dividing the volumetric ammonium removal rate obtained in the experiments performed without carriers by that obtained with both attached (biofilm) and suspended solids. The remaining amount (calculated by subtracting the percentage attributed to suspended solids from 100%) was credited to attached biomass activity. Biomass-specific ammonium removal rates (here also referred to as specific nitrifying activity) obtained with either attached or suspended biomass was determined by the ratio between the volumetric ammonium removal rate obtained with each fraction of biomass and the corresponding amount of solids (either VAS or VSS).

2.3. Scanning electron microscopy (SEM) analysis of the attached biomass

The properties of the biomass attached to the carrier elements (e.g., biofilm thickness) of both MBBR systems were evaluated by SEM. This analysis was carried out during run 4, condition in which the volumetric organic loading rate reached the maximum value (Table 1). For visualization of the adhered biomass, a piece of the Kaldnes K1 (MBBR$_1$) and Mutag Biochip (MBBR$_2$) carriers was cut by means of a razor blade. This procedure was performed very carefully to keep the biofilm structure unchanged. The preparation of the sample (i.e., fixation, post-fixation, dehydration, washing and drying) can be found elsewhere (Bassin et al., 2012a). The prepared specimen was further attached to supports (aluminium stubs) with the aid of silver glue and finally coated with gold powder in a Balzers FL-9496 metalizer for observation in a Jeol JSM-6340F microscope. The biomass thickness could then be determined by the tools provided by the microscope software.

2.4. Analytical measurements and calculation procedures

COD, ammonium, total suspended solids (TSS) and volatile suspended solids (VSS) were determined according to Standard Methods (Apha, 2005). Nitrite and nitrate were measured by analytical test kits provided by Hach Co. (Loveland, Colorado, USA). The biomass concentration in the carrier media, expressed as total (TAS) and volatile (VAS) attached solids, was measured according to the procedure described

previously (Bassin et al., 2012a), with minor modifications. Three representative carriers of each reactor were collected and placed in a falcon tube. A known volume of a 1 N NaOH solution was then added to the tubes to aid the removal of the attached biomass from the carrier materials. Subsequently, the detached biomass present in the aqueous solution was quantified following the same procedure used to determine the suspended solids concentration (Apha, 2005). The amount of NaOH solids remaining after the biomass determination procedure was subtracted from the total amount of solids in the sample aliquot. In order to extrapolate the results obtained in this determination for the entire reactor and therefore calculate the TAS and VAS concentrations (g/L), the total number of plastic carriers within the MBBRs and the volume of the bioreactors were taken into account. The sum of volatile attached (VAS) and suspended solids (VSS) was designated as total volatile solids (VTS). Dissolved oxygen levels were regularly monitored with a WTW DO meter (model Oxi 7310). Temperature and pH were measured by means of a Oakton pH 110 meter. Total polysaccharides (PS) and protein (PT) concentrations of the biomass attached to the plastic carrier elements were also determined. For PS and PT determination assays, two representative carriers from each reactor were placed in a falcon tube, to which a solution of 1 N NaOH was added. The tubes were heated during 5 min at 90 °C in order to promote complete cell lysis. Subsequently, PS concentration was measured according to Dubois et al. (1956) whereas PT concentration was determined by the Bradford assay (Bradford, 1976). Nitrogen mass balance was conducted by considering the influent nitrogen (as ammonium) and the effluent nitrogen (as remaining ammonium and nitrite and nitrate formed by nitrification). The total amount of influent ammonium which was found back as nitrate/nitrite in the bulk liquid was designated as soluble nitrogen conservation whereas the difference between those two was referred to as total nitrogen removal. Nitrogen was considered to account for about 10% of the cell dry weight (Gerardi, 2003). Given that biofilm development is a dynamic process governed by attachment and detachment of biomass to solid surfaces, the biofilm surface specific detachment rate (k_d) was calculated. Calculations procedures are shown in Supplementary material.

3. Results

3.1. General description of the reactors operation: COD removal and nitrogen conversions at different organic loading rates

After inoculation of the reactors with activated sludge from a municipal wastewater treatment plant, around 20 and 30 days were necessary to achieve constant attached biomass concentration in MBBR$_1$ and MBBR$_2$, respectively. This period is referred to as start-up phase, during which the plastic carriers were being colonized by the microorganisms at the initially applied organic loading rate (0.8 kgCOD/(m^3 d)) (Table 1). With the exception of this transient period, COD removal was observed to be higher than 90% in both reactor systems (Fig. 1). Despite the gradual increase in the organic loading rate from 0.8 kgCOD/(m^3 d) (run 1) to 3.2 kgCOD/(m^3 d) (run 4), COD removal was observed to be above 95% in both MBBRs. From runs 4–6, period during which the organic loading rate was kept constant at 3.2 kgCOD/(m^3 d) (12.8 gCOD/(m^2 d)) by proportionally decreasing the influent COD and the HRT, the performance of both systems in terms of organic matter
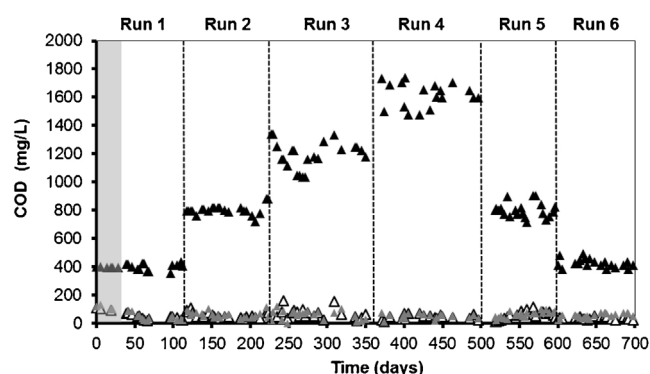

Fig. 1 – Influent (▲) (equal for both reactors) and effluent COD over the continuous operation of MBBR$_1$ (▲) and MBBR$_2$ (△). The grey shaded area within Run 1 refers to the start-up phase (20 and 30 days for MBBR$_1$ and MBBR$_2$), period during which the biofilm was formed in the freely moving carriers. The varying operational conditions applied over time were the same for both reactors. From runs 1–4, the organic loading rate was gradually increased by increasing the influent COD. Subsequently (runs 4–6), both the COD concentration in the incoming wastewater and the HRT were proportionally reduced to maintain the COD loading rate constant at 3.2 kgCOD/(m^3 d) (or 12.8 gCOD/(m^2 d)).

removal remained stable, as indicated by the high COD removal obtained within this period.

Ammonium profiles in the influent and effluent of MBBR$_1$ and MBBR$_2$ are shown in Fig. 2. During the biofilm formation period within run 1, ammonium removal was slightly higher in the reactor filled with Kaldnes K1 media (MBBR$_1$) in comparison with that containing Mutag Biochip carriers (MBBR$_2$). Nevertheless, after 40 days of operation, nearly complete ammonium removal was obtained in both reactors, regardless of the carrier material used. Despite the gradual increase in the organic loading rate from 0.8 kgCOD/(m^3 d) (run 1) to 3.2 kgCOD/(m^3 d) (run 4), nitrification performance remained very stable, as demonstrated by the high ammonium removal (>90%) achieved within this period. On the other hand, the reduction of HRT from 12 to 6 h and consequent increase in
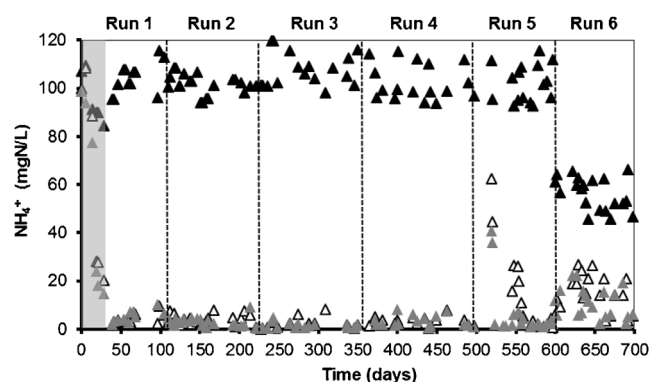
Fig. 2 – Influent (▲) ammonium (equal for both reactors) and effluent ammonium concentrations profiles over the course of the operation of MBBR$_1$ (▲) and MBBR$_2$ (△). The grey shaded area within run 1 refers to the start-up phase, during which the biofilm was establishing in the carrier elements. The influent ammonium concentration in run 6 was half of that applied in the previous runs. However, the nitrogen loading rate was kept constant by reducing the HRT from 6 to 3 h.

(a) MBBR$_1$ (Kaldnes K1 carriers) (b) MBBR$_2$ (Mutag Biochip carriers)
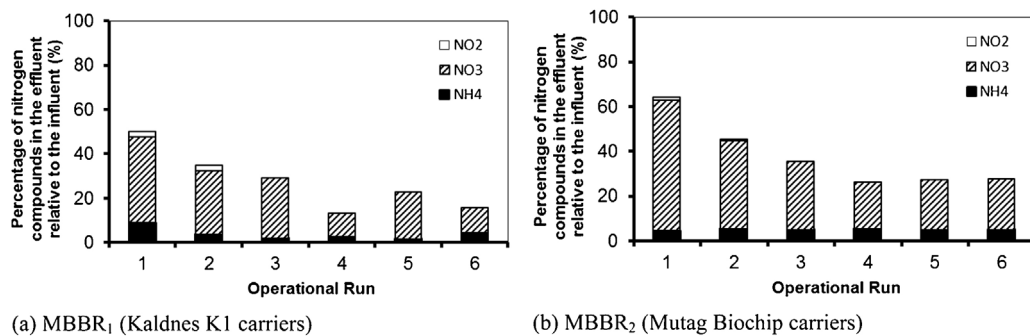
Fig. 3 – Average fraction of ammonium, nitrite and nitrate found in the effluent relative to the total influent nitrogen (entirely as ammonium) over the 6 experimental runs. The amount of soluble nitrogen which was not found back in the effluent (i.e., not conserved within the system) was either used for biomass growth or lost to the atmosphere in the form of nitrogen gas resulting from denitrification.

the nitrogen loading rate from 0.2 to 0.4 kgNH$_4$$^+$–N/(m^3 d) in the transition from run 4 to 5 was accompanied by ammonium concentration peaks in the effluent of both reactors, which reflected a drop in the ammonium removal (Fig. 2). The impact of the lower HRT on nitrification was felt most in MBBR$_2$, where it took 60 days to re-establish full ammonium conversion. On the other hand, only 20 days were necessary to reach effluent ammonium concentrations of about 1 mgN/L in MBBR$_1$ after the hydraulic shock loading. Ammonium removal was also observed to be negatively influenced with a second decrease in the HRT occurred in run 6, even though both the organic and nitrogen loading rate were the kept the same as in the previous experimental condition (run 5).

The nitrogen conversions taking place in the MBBRs can be better visualized in Fig. 3, where the percentage each nitrogen compound in the effluent (as remaining ammonium or nitrate/nitrate resulting from nitrification) relative to the influent nitrogen (entirely as ammonium) is displayed. Further information on the influent and effluent total nitrogen concentrations in each experimental stage can be found in Fig. S2.

In both reactors, nitrate accounted for the majority of the nitrogen in the output stream whereas nitrite was only detected in minor amounts (less than 2%). Furthermore, the total amount of soluble nitrogen found in the effluent was observed to decrease from runs 1 to 4. However, within the period during which the organic loading rate was kept constant (runs 4–6), only a slight variation in the effluent nitrogen was observed in the two reactors. In fact, as the organic loading rate was gradually increased in the first four experimental

conditions, the amount of nitrogen used for biomass synthesis became more relevant. Consequently, less ammonium was available for nitrification and the amount of oxidized nitrogen (nitrate/nitrite) generated has therefore diminished, contributing to decrease the nitrogen conservation in the bulk. Furthermore, by considering the amount of soluble nitrogen present in the effluent (as ammonium, nitrite and nitrate) and that expected for fully aerated nitrifying reactors with no anoxic zones intentionally implemented (calculated by subtracting the nitrogen used for biomass growth from the total nitrogen fed), 20 to 40% of nitrogen was still missing. Possibly, this amount of nitrogen was lost to the atmosphere in the form of nitrogen gas resulting from denitrification, as will be discussed further on. Taking into account the influent and effluent measurements, total nitrogen removal was observed to vary from 50 to 86% in MBBR$_1$ and from 35 to 73% in MBBR$_2$.

3.2. Attached and suspended biomass fractions

The dynamics of the volatile suspended and attached biomass over the six experimental stages is displayed in Fig. 4. For comparison with the amount of biomass present in suspension, the sludge adhered to the carriers was also expressed in g/L. In MBBR$_1$, the attached biomass concentration gradually increased from 3 gVAS/L (run 1) to 5.5 gVAS/L (run 4) as the organic loading rate was raised. Within the period in which the organic load was kept constant (runs 4–6), it remained relatively constant at around 6 gVAS/L (Fig. 4a). Even though the media filling fraction was chosen to have the same theoretical surface area for biofilm growth in both reactors, average

(a) MBBR$_1$ – Kaldnes K1 carriers (b) MBBR$_2$ – Mutag Biochip carriers
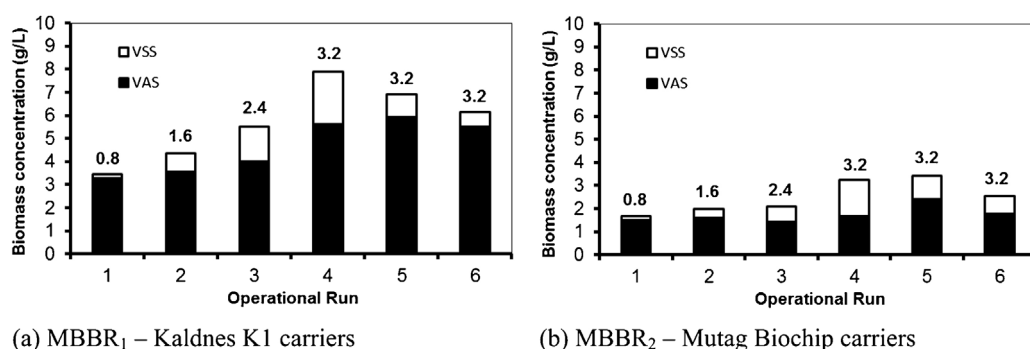
Fig. 4 – Average attached (VAS) and suspended (VSS) biomass concentrations in MBBR$_1$ (a) and MBBR$_2$ (b) obtained in each operational condition. The number above the bars indicates the volumetric organic loading rate applied in each experimental stage. The same y-axis scale was used in (a) and (b) for better comparison between the results of each system.
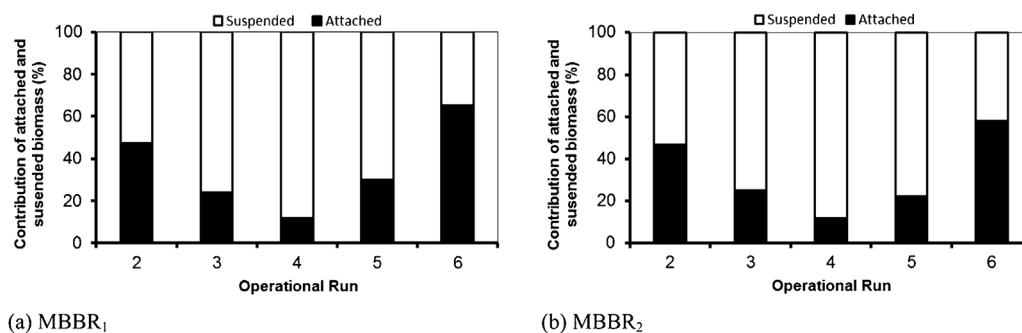
(a) MBBR$_1$ (b) MBBR$_2$

Fig. 5 – Contribution of the attached and suspended biomass to the overall ammonium removal, as estimated from the batch tests. (a) MBBR$_1$ (Kaldnes K1) and (b) MBBR$_2$ (Mutag Biochip).

attached biomass content in the Mutag Biochip carriers of MBBR$_2$ only amounted to around 1.5 gVAS/L (Fig. 3b). Furthermore, unlike that observed in MBBR$_1$, adhered solids in the supports of MBBR$_2$ only slightly increased as the organic loading rate was increased. The comparison between the quantity of attached biomass per m^2 of support for the two different media is illustrated in Fig. S3. The average surface biomass content in MBBR$_1$ (around 18 g/m^2) was found to be approximately 2.5 times higher than in MBBR$_2$ (around 7 g/m^2). Inert material (fixed solids) in the biofilm of MBBR$_1$ and MBBR$_2$ only accounted for about 15% and 10% of the total attached solids, respectively.

It is also important to note that, particularly in the Kaldnes K1 carriers, great part of the biomass was not effectively attached to the support, but entrapped with the biomass fixed to it (Fig. S4). From the SEM analysis, the thickness of the biofilm effectively adhered to this particular media was observed to be around 1.2 mm (Fig. S4a). On the other hand, the porous structure of the Mutag Biochip carrier made this determination more difficult to be accomplished for this support. In fact, only a very thin layer of biomass was observed in the surface of this media, whereas a considerable amount of solids were found inside the pores located along the depth of the carrier (Fig. S4b). Interestingly, at this specific location, the biomass appeared in the form of dense agglomerates, not covering the whole pore space. Given the possible inaccuracy of the biofilm thickness measurements for this porous carrier, no absolute value is reported. Nevertheless, by considering the maximum nominal length of the carrier (Table S1) and the fact that biomass was distributed mainly inside the pores, a biofilm layer lower than 0.8–1.2 mm can be expected.

As regards to the volatile suspended solids (VSS), it represented only a fraction of 10% of the total volatile solids (VAS + VSS) at the lowest organic load (run 1) in both reactors (Fig. 4). However, further increase in the COD loading rate from runs 1–4 was accompanied by a considerable increase in amount of bulk phase biomass in both systems. In run 4, in which the organic loading rate reached the highest value (3.2 kgCOD/(m^3 d)), VSS accounted for 28% of the total amount of biomass in MBBR$_1$, whereas this fraction reached up to 48% in MBBR$_2$, practically equalling the amount of solids attached to the media (Fig. 4b). At this particular condition, the plastic carriers of both reactors exhibited the thickest biofilm and were completely saturated with biomass (see Fig. S4). With the decrease of HRT from runs 4–6, the amount of VSS was observed to decline as a result of biomass washout, although the organic loading rate was kept constant within this period. The percentage of inert biomass within the TSS was around 25% and 21% in MBBR$_1$ and MBBR$_2$, respectively.

The biofilm surface specific detachment rate (k_d) was calculated for each operational run and the results are shown in Fig. S5. Overall, as the COD loading rate was increased from runs 1–4, a pronounced increase was observed in k_d, reflecting an increase in the amount of suspended solids which were sheared from the carriers. k_d value was kept within 0.3 and 2.4 gVSS/(m^2 d) in MBBR$_1$ and 0.2 to 2.4 gVSS/(m^2 d) in MBBR$_2$.

### 3.3. Polysaccharides and protein concentrations in the biofilm

Given the importance of polysaccharides (PS) and proteins (PT) as structuring agents of the biofilm, the concentrations of these polymeric substances in the attached biomass were regularly determined over the operation of the reactors. Following the trend observed for the adhered solids, higher PS and PT contents were found in the biofilm of MBBR$_1$ in comparison with MBBR$_2$ (Fig. S6). However, PT/VAS and PS/VAS ratios for both MBBRs were observed to be very similar throughout the experimental runs. Furthermore, PS/PT ratio remained practically constant at around 0.4 from runs 1–4. As the HRT was gradually reduced in runs 5 and 6, the increase of PS content was more pronounced than that of PT. Hence, PS/PT ratio gradually increased, reaching up to 0.55 (MBBR$_1$) and 0.6 (MBBR$_2$) in the last experimental stage. During this period, the biofilm of both reactors experienced an overproduction of gelatinous polymeric substances (see Fig. S7 for more details).

3.4. Nitrifying activity tests

The batch tests were initially conducted to observe the influence of the increasing organic loads on the maximum biomass specific nitrifying activity. With the enhanced heterotrophic growth resulting from the gradual increase of the influent organic load (runs 1–4), the specific ammonium removal rate gradually decreased (Fig. S8). Subsequently, at constant COD loads (runs 4–6), it varied within the range of 1.2–2.3 mgNH$_4$–N/(gVTS h) (in MBBR$_1$) and 3.0–5.6 mgNH$_4$–N/(gVTS h) (in MBBR$_2$).

Taking into consideration the considerable amount of suspended solids observed especially from run 2 onwards (Fig. 4), batch experiments were conducted with and without the carriers to separately estimate the amount of ammonium oxidized either by the attached or by the suspended biomass (details of the calculation procedures can be found in Section 2). The volumetric ammonium removal rates obtained with each type of biomass is presented in Table S2. Interestingly, on basis of the activity batch tests results, it could be inferred that the contribution of the suspended biomass to the total
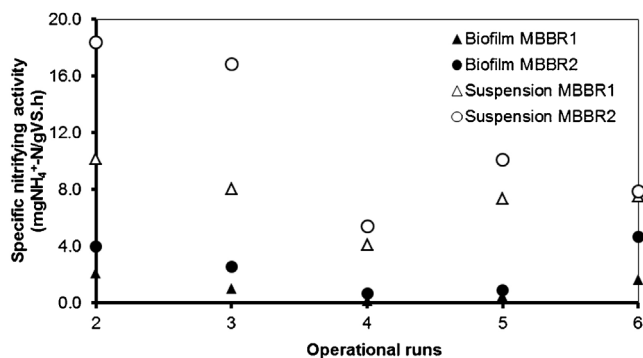
Fig. 6 – Specific ammonium oxidation rates obtained with the attached (biofilm) and suspended biomass in MBBR$_1$ and MBBR$_2$ from runs 2–6. The data representing run 1 is not shown since the activity batch test was not conducted for this particular experimental condition.

nitrifying activity was very pronounced (Fig. 5). Furthermore, the amount of ammonium estimated to be nitrified by the bulk phase biomass becomes even more significant as the organic loading rate increased at constant HRT (runs 2–4). In run 4, when the highest concentration of suspended biomass was observed in both reactors (Fig. 4), the amount of ammonium removed by the suspended biomass was estimated to account for around 85% of the total ammonium removed in both reactors (Fig. 5). In order to evaluate how the relative importance of the suspended biomass to the overall ammonium removal is affected by the HRT, this parameter was gradually reduced from 12 h (run 4) to 6 h (run 5) and subsequently from 6 h (run 5) to 3 h (run 6), while the organic loading rate was kept constant by decreasing the influent COD accordingly. As it can be seen, the fraction of the influent ammonium estimated to be removed by the suspended solids gradually decreased reaching a minimum value of 35% (MBBR$_1$) and 42% (MBBR$_2$) in run 6.

Besides the important role played by the bulk phase solids in the nitrification process, the specific nitrifying activity of the suspended biomass (VSS) was observed to be considerably higher than that of attached biomass (VAS) in both reactors (Fig. 6). The VSS-specific nitrification rate reached up to 20 and 11 times higher than the VAS-specific nitrification rate in MBBR$_1$ and MBBR$_2$, respectively. Nevertheless, a great increase in the specific nitrifying activity of the biofilm was noticed as the HRT was decreased to 3 h in run 6. This result coincides with the higher fraction of ammonium oxidized by the attached biomass under this particular experimental condition (Fig. 5). In general, both the attached and suspended biomass-specific nitrifying activities were observed to be higher in MBBR$_2$ than in MBBR$_1$, and tended to decrease as the COD load was increased at constant HRT (runs 2–4). Furthermore, the performance of the reactor filled with Mutag Biochip media was very comparable to that of MBBR$_1$, despite the lower attached biomass concentrations observed in this reactor.

4. Discussion

4.1. Effect of carrier type on attached biomass accumulation and biofilm sloughing at increasing COD loading rates

From literature it is known that the key factor for the design of moving-bed biofilm reactors is the effective surface area available for biomass growth (Ødegaard et al., 2000; Ferrai

et al., 2010). In this context, once the specific surface area is known for a given carrier, its size and shape are usually not important for design purposes (Ødegaard et al., 2000). In this study, the media filling ratio was chosen in order to have the same theoretical specific area for biofilm growth in both reactors. Due to this fact and taking into account that the two MBBRs were always subjected to the same feeding pattern over time, similar attached biomass concentrations were expected in both systems. However, it was observed that the Kaldnes K1 carriers (media used in MBBR$_1$) allowed obtaining higher attached biomass concentrations compared to those reached in MBBR$_2$, where the Mutag Biochip was employed as support media (Fig. 4 and Fig. S3). These findings suggest that the amount of attached biomass which can be achieved in a MBBR system does not only depend on the theoretical biofilm surface area shown by the support material, but also on the carrier configuration. The Mutag Biochip carriers present in MBBR$_2$ have a parabolic shape which is frequently subjected to shear forces and attrition due to intensive contact with the surrounding liquid and with other media. These conditions favour the detachment of biofilm and the amount of attached solids tends to decrease. On the other hand, the Kaldnes K1 media consist of cylindrical-shaped carriers which have a protected surface area in its inner part which is not subjected to direct collision with other particles, favouring the accumulation of biofilm. Furthermore, this media configuration also facilitates the entrapment of biomass in the biofilm matrix, as observed in this study (Fig. S4), while the Mutag Biochip does not. Consequently, the amount of attached solids which can be achieved in the former support is enhanced. However, it should be pointed out that the entrapped biomass portion found in the protected zone of the Kaldnes K1 carriers was only loosely bound to the biofilm and therefore much more susceptible to detachment than the solids effectively attached to the plastic media. This may explain the huge increase in the biofilm loss rate observed in MBBR$_1$ as the applied organic loading rate was increased (Fig. S5).

Another point which should be considered is that the surface area of the carrier provided by manufacturers may change over time due to the overgrowth of biofilm and consequent media clogging (Forrest, 2014). Contrary to the Kaldnes K1 media, the Mutag Biochip carrier is a fine porous chip-type media in which microorganisms form colonies in the protected pores. Although the theoretical volume-specific surface area of this carrier is reported to be 3000 m^2/m^3, it might be possible that the effective area for biofilm growth decreases as biomass attaches to the media. This may also explain the lower attached biomass content found in MBBR$_2$. Overall, these outcomes suggest not only the specific area for biofilm attachment of the support media but also its characteristics (shape, size and surface) should be taken into account for the design and operation of MBBR systems.

MBBRs usually present relatively low amount suspended solids in the effluent, commonly within the range of 150–250 gSS/m^3 (Ødegaard et al., 2010). Consequently, easier biomass-effluent separation can be achieved in such biofilm systems in comparison to conventional suspended growth reactors. However, the effluent of high organic loaded MBBRs may contain significant amounts of biomass in the bulk phase, as observed previously (Melin et al., 2004). In the current study, it was observed that at the highest surface organic load applied (around 13 gCOD/(m^2 d)), the carriers of both systems were completely saturated with biomass and got clogged. As a result, the specific surface detachment rates increased,

leading to a higher amount of suspended solids. For instance when HRT and the organic loading rate were set at 12 h and 3.2 kgCOD/(m^3 d) (run 4), respectively, the VSS concentration reached up to 2.3 g/L in MBBR$_1$. This value is actually within the normal range observed in conventional activated sludge reactors (Metcalf and Eddy, 2003). Excessive biofilm thickness has been already reported to potentially lead to sloughing events and elevated effluent suspended solids concentrations (Downing et al., 2013). Given the considerable amount of solids in suspension resulting from biofilm detachment in the high loaded MBBRs and taking into account that the characteristics (e.g., particle size, composition, texture and morphology) of the biomass sloughed-off from MBBR carriers are different from flocculent activated sludge (Nof et al., 2013), the clarifying unit should be specifically designed to meet the effluent quality requirements.

The excessive production of gelatinous exopolysaccharides by the microorganisms (Fig. S7) and consequent increase of biofilm PS/PT ratio (Fig. S6) observed in run 6 was an unexpected observation, as no similar event had been observed in the two previous stages subjected to the same organic loading rate (runs 4 and 5). Therefore, it is speculated that this finding can be interpreted as a response of the biomass in an attempt to not be washed out from system at the lowest HRT applied. Nevertheless, regardless of its main causes, the results suggest that under constant organic loads, the hydraulic conditions may induce changes in bacterial behaviour. It is relevant to mention that the particular episode of exopolymers overproduction noticed in this study may affect some of the sludge properties, such as its settleability. In those circumstances, the use of chemical coagulants can be an option to improve effluent clarification (Ødegaard, 2006; Ødegaard et al., 2010).

4.2. *Effect of increasing organic loading rates and carrier type on organic matter removal, nitrification and specific nitrifying activity*

The long-term experiment in which the two MBBRs were compared side-by-side for 700 days has shown that both systems could accommodate increasing COD loading rates up to 12.8 gCOD/(m^2 d). Running a lab-scale MBBR system at similar surface organic loads, Aygun et al. (2008) also observed high organic matter removal efficiency (close to 95%). Javid et al. (2013) operated a MBBR process subjected to surface organic loading rates varying from 2.4 to 11.6 gBOD$_5$/(m^2 d), which is within the range applied in this study. The performance of the reactor was kept stable even at the highest load applied and a high effluent quality was achieved over the entire operation. Overall, the efficacy of MBBRs in tolerating increasing organic loads is well reported in literature. However, little research has been undertaken on the effect of different media on their performance under high COD input.

In this study, the type of carrier used in each reactor did not impact the overall performance of the system. Even though the attached solids concentration in MBBR$_2$ was lower than that observed in MBBR$_1$, organic matter and ammonium removal were similar in both systems under the experimental conditions employed. First, one can consider that this result is possibly related to the biomass distribution pattern over the two different media, which present distinct shape, size and surface characteristics. In MBBR$_1$, the largest fraction of biomass was located at the inside of Kaldnes K1 carriers (Fig. S4), which were observed to be completely clogged at the highest organic load. Furthermore, as evidenced by SEM analysis,

the thickness of the biofilm adhered to the supports in MBBR$_1$ was observed to be very significant (about 1.2 mm). Under such conditions, the free passage of nutrients and oxygen through the attached biomass layer is restricted, subjecting the inner parts of the biofilm to substrate- and oxygen-limited conditions. As reported in previous studies, the biofilm zones near the substratum are potentially colonized by inert biomass (Zhang and Bishop, 1994). This is especially the case of thick microbial films as those observed in the Kaldnes K1 media, in which the amount of viable biomass may decrease considerably from the outer surface to the bottom of the biofilm (Zhang and Bishop, 1994). On the other hand, the biomass attached to the flat disk-type Mutag Biochip carriers in MBBR$_2$ was mainly distributed as a substantially thin layer over the surface of both sides the carriers or in the form of agglomerates growing inside their pores (Fig. S4). As the nutrients and oxygen could reach the biofilm from the two sides of the media, the transport of these elements through the attached bacteria was facilitated. Indeed, the fraction of inert material in the biofilm of MBBR$_2$ was observed to be lower than that of MBBR$_1$. Moreover, the specific biofilm activity (assessed from ammonium oxidation experiments) in MBBR$_2$ was higher than in MBBR$_1$ (see Fig. 6), compensating for the lower amount of solids attached to the media. Hence, from a conversion point of view, the results suggest that it is more important to maximize the active biofilm surface area within the reactor than the total attached biomass content.

However, apart from the influence of the media type on attached biomass distribution in the carrier and the consequent role played by the support on the biofilm conversions, the results also suggested that there were other factors affecting the overall performance of the MBBRs which should be considered to explain our findings. As previously described, both systems have shown stable nitrification and full ammonium removal even at most extreme condition of organic load, although they presented significantly different attached biomass contents. It is well known that nitrification is directly influenced by the applied organic loading rate, with high COD loads favouring the development of fast-growing heterotrophs (Rittmann and Manem, 1992). As autotrophic nitrifiers compete poorly for oxygen and nutrients, especially in high loaded attached growth processes, they tend to be overgrown by heterotrophic organisms (Figueroa and Silverstein, 1992; Ohashi et al., 1995). Under such conditions, nitrifiers are potentially forced deeper into the biofilm, where a greater mass transport resistance is experienced (Rittmann and Manem, 1992). Hence, nitrification in the biofilm may be negatively impacted. As presented before, at the highest organic load applied in this study (3.2 kgCOD/(m^3 d)), the plastic carriers were completely saturated with heterotrophic biomass and got clogged, making the diffusion of oxygen and substrate through the biofilm more difficult. Herewith, a harsh environment was created to sustain nitrifying activity in the biofilm and a sharp decrease in the nitrification performance was expected. Nevertheless, high ammonium removal levels were sustained in both MBBRs. As the suspended solids became very relevant as the COD load was gradually increased, reaching similar amounts in both systems (Fig. 4), we suspected that the bulk phase biomass could have been directly involved in the nitrogen conversions.

Moving-bed biofilm reactors are usually operated at low HRTs (Ødegaard, 2006) which are theoretically not sufficient to support the growth of slow growing nitrifying organisms in suspension. Depending on site-specific conditions, nitrifiers

usually present maximum specific growth rates ranging from 0.25 to 0.77 d^{-1} (Randall et al., 1992). Considering the reciprocal of the average of these two values (i.e., 0.51 d^{-1}), the HRT necessary to allow nitrifiers to grow in the mixed liquor phase was calculated to be around 2 days (48 h). In our study, the HRT was initially set at 12 h, being subsequently reduced to 6 and 3 h. Presumably, under these conditions, the suspended growth of nitrifiers would be hindered and nitrifying activity is expected to occur mainly in the biofilm. However, a recent work conducted by Piculell et al. (2014) has shown that there was always some suspended biomass in MBBRs as a result of biofilm sloughing, even at washout conditions. Furthermore, following the same line of reasoning, Mašic and Eberl (2014) have shown by mathematical modelling that suspended biomass always contributes to ammonium removal in biofilm systems. These authors pointed out that neglecting the contribution of non-attached biomass leads to quantitatively different results. Earlier studies reported that in hybrid moving-bed biofilm-activated sludge processes (usually referred to as integrated fixed-film activated sludge—IFAS), the fraction of ammonium which is oxidized by the suspended biomass may account for 10–70% of the overall nitrification (Albizuri et al., 2014). On the other hand, studies reporting the operation of pure moving-bed reactors often neglect the activity of nitrifiers in the bulk phase, assuming that nitrification only takes place in the biofilm (Piculell et al., 2014).

In our study, we observed that the dynamics of suspended and attached biomass fractions was substantially influenced by the COD input. The experiment has started with two pure MBBR systems in which the suspended solids accounted for only 4–5% of the total biomass content. However, as the organic loading rate was increased, the amount of dispersed biomass resulting from biofilm sloughing became very significant, reaching up to 26% and 43% of the total biomass content in $MBBR_1$ and $MBBR_2$, respectively. Under such conditions, the bulk solids content became closer to those found in hybrid bioreactors relying on both suspended and attached biomass growth (Bellucci et al., 2013). Given this scenario, nitrifying activity batch tests were conducted to evaluate the role of the suspended bacteria on the nitrification process. Indeed, the results have revealed that the fraction of ammonium estimated to be nitrified by the bulk phase solids was very significant, and increased proportionally to the applied organic loading rate at invariable hydraulic conditions (i.e., constant HRT). Under high organic load conditions, biofilm detachment rates became more relevant, contributing to seed the suspension with nitrifiers. Since the mixed liquor phase is not affected by mass transfer limitations to the same extent as the biofilm, the suspended biomass-specific nitrifying activity was found to be much higher than that of the attached biomass (Fig. 6). Thus, as the COD loading rate was raised, the increasing percentage of ammonium oxidized in suspension may have compensated for the decreasing nitrifying activity of the biofilm. This, in turn, allowed both MBBRs to achieve stable nitrification even when subjected to increasing organic loads.

The results also indicated that at constant organic loading rates (e.g., runs 4–6), the HRT directly affected the amount of ammonium oxidized either by the suspended or attached biomass. Similarly to earlier investigations concerning the operation of MBBR systems (Piculell et al., 2014), the amount of solids in suspension was observed to decrease as the HRT was reduced. Consequently, the relative importance of suspended biomass to the biological conversion processes (e.g.,

nitrification) decreased. Furthermore, the significant washout of bulk solids with relatively high nitrifying activity adversely affected nitrification performance in the high loaded MBBRs. This was clearly observed under the lowest HRT applied (run 6), when complete nitrification was never achieved (Fig. 2), even though the organic and nitrogen loading rate were the same as those applied in run 5. This particular result emphasizes the importance of the suspended biomass to the overall ammonium removal obtained in both reactors.

It is also interesting to note that, as demonstrated by the batch experiments, the specific nitrifying activity of the suspended biomass was quite higher than the respective biofilm activity, while both tended to decrease with the increasing COD load. However, it should be remarked that the attached biomass-specific nitrification rate increased at the lowest HRT (run 6), although the applied volumetric organic loading rate was kept the same as in the two previous experimental runs (Fig. 6). This finding is probably due to the higher washout of suspended solids occurred in this particular condition, enabling a greater amount of ammonium to be nitrified by the attached biomass (Fig. 5). In turn, the VAS-specific activity has raised considerably. In terms of surface nitrification rates, the maximum values were found to be 0.87 and 0.80 gNH_4–$N/(m^2 d)$ in $MBBR_1$ and $MBBR_2$, respectively. Besides reporting slightly higher surface nitrification rates (0.9–1.2 gNH_4–$N/(m^2 d)$) in a hybrid activated sludge-biofilm reactor treating municipal wastewater, Christensson and Welander (2004) observed that more than 80% of the overall nitrification was performed by the biofilm. However, it should be considered that their experiments were conducted in lower COD loading ranges. Operating a hybrid bioreactor containing porous ceramic particles as support media, Wang and Wu (2004), reported that both bulk and attached biomass exhibited fairly similar nitrification activity. Their experiment was, however, conducted on autotrophic conditions, with no carbon source present in the synthetic influent medium. On the other hand, in our study, massive growth of heterotrophic organisms in both attached and suspended phases was observed as a result of the high COD loading rates. Thus, the relative importance of the nitrifying population within the overall bacterial community became significantly smaller, while the specific nitrification rates tended to decrease.

4.3. The role of the media type on total nitrogen removal

Although the MBBR systems under study were continuously kept under aeration and therefore only designed to accomplish COD removal and nitrification, high total nitrogen removal was observed (up to 86 and 73% in $MBBR_1$ and $MBBR_2$, respectively). Partially, this was due to the increasing fraction of the incoming nitrogen assimilated by heterotrophic bacteria for cell synthesis as COD loading rate was raised. Therefore, the amount of nitrogen available to be nitrified has decreased and a higher soluble nitrogen loss was noted (Fig. 3). Furthermore, part of the influent nitrogen which was not found back as oxidized nitrogen (nitrite and nitrate) or residual non-nitrified ammonium was possibly removed via denitrification. Even though only aerobic conditions prevailed in the bulk liquid (DO ranging from 4 to 5 mg/L), the thick biomass layer established in the carrier media of $MBBR_1$ and $MBBR_2$ possibly resulted in oxygen mass transport limitation and enabled the establishment of anoxic conditions in the inner zones of the biofilm, where denitrification could take place. This also

may explain the increasing gap in the soluble nitrogen balance observed from runs 1–4 in both reactors, period when the biofilm thickness has become increasingly larger. Moreover, although both reactors were always subjected to the same operational conditions over time, higher nitrogen removal was observed in the reactor filled with Kaldnes K1 media (MBBR$_1$) (Fig. 3). Taking into account that the amount of nitrogen used for growth was similar in both systems, the higher nitrogen loss observed in MBBR$_1$ is possibly due to the higher thickness of the biofilm grown in protected surface area of the carrier, favouring the development of anoxic environment. On the other hand, the flat-disk Mutag Biochip carriers (media of MBBR$_2$) show a conformation which favours the diffusion of oxygen through the biofilm from both sides of the porous media, making the establishment of anoxic conditions and the occurrence of denitrification less likely to occur.

As reported in previous studies (Matsumoto et al., 2007), the results derived from our experiments suggest simultaneous nitrification and denitrification (SND) can be accomplished in attached-growth reactors kept under high bulk oxygen concentration with no deliberate anoxic phase, provided that the biofilm is sufficiently thick. Furthermore, the magnitude of SND and the associated nitrogen removal are dependent on the specific carrier type. These observations stress the need for considering not only the effective surface area but also the configuration of the media (e.g., size and shape) and the biofilm characteristics (thickness and biomass content) in the mathematical modelling of moving-bed biofilm reactors for better description of the biological conversions and specific microbial activities along with the prediction of the effluent quality.

5.   Conclusions

High COD and ammonium removal were observed in two MBBRs at organic loads up to 3.2 kgCOD/(m^3 d), regardless of the support media used in each reactor. However, the type of carrier directly impacted the distribution and amount of attached biomass. As the COD input was increased at constant HRT, the amount of suspended solids became considerably higher. Batch experiments have shown that, besides exhibiting relatively higher nitrifying activity as compared to the biofilm, the bulk phase biomass played an important role in the overall nitrification process. At constant organic loads, nitrification performance was affected by the applied HRT, as it directly influenced the suspended and attached solids dynamic profiles and therefore the fraction of ammonium oxidized by each biomass fraction. Appreciable total nitrogen removal was achieved indirectly as a result of both nitrogen assimilation by heterotrophs and denitrifying activity in the inner (anoxic) layer of the biofilm, despite the maintenance of high bulk oxygen concentrations in both reactors.

Acknowledgments

Appendix A. Supplementary data

Supplementary data associated with this article can be found, in the online version, at http://dx.doi.org/10.1016/j.psep.2016.01.007.

References

Albizuri, J., Grau, P., Christensson, M., Larrea, L., 2014. Validating the colloid model to optimize the design and operation of both moving-bed biofilm reactor and integrated fixed-film activated sludge systems. Water Sci. Technol. 69, 1552–1557.

Apha, 2005. Stardand Methods for the Examination of Water and Wastewater, 21st ed. American Public Health Association, American Water Works Association, Water Environmental Federation, Washington, DC.

Aygun, A., Nas, B., Berktay, A., 2008. Influence of high organic loading rates on COD removal and sludge production in moving bed biofilm reactor. Environ. Eng. Sci. 25, 1311–1316.

Barwal, A., Chaudhary, R., 2014. To study the performance of biocarriers in moving bed biofilm reactor (MBBR) technology and kinetics of biofilm for retrofitting the existing aerobic treatment systems: a review. Rev. Environ. Sci. Biotechnol. 13, 285–299.

Bassin, J.P., Dezotti, M., Sant'Anna Jr., G.L., 2011. Nitrification of industrial and domestic saline wastewaters in moving bed biofilm reactor and sequencing batch reactor. J. Hazard. Mater. 185, 242–248.

Bassin, J.P., Kleerebezem, R., Dezotti, M., van Loosdrecht, M.C., 2012a. Simultaneous nitrogen and phosphate removal in aerobic granular sludge reactors operated at different temperatures. Water Res. 46, 3805–3816.

Bassin, J.P., Kleerebezem, R., Rosado, A.S., van Loosdrecht, M.C.M., Dezotti, M., 2012b. Effect of different operational conditions on biofilm development, nitrification, and nitrifying microbial population in moving-bed biofilm reactors. Environ. Sci. Technol. 46, 1546–1555.

Bellucci, M., Ofiteru, I.D., Head, I.M., Curtis, T.P., Graham, D.W., 2013. Nitrification in hybrid bioreactors treating simulated domestic wastewater. J. Appl. Microbiol. 115, 621–630.

Bradford, M.M., 1976. Rapid and sensitive method for the quantitation of microgram quantities of protein utilizing the principle of protein-dye binding. Anal. Biochem. 72, 248–254.

Boltz, J.P., Johnson, B.R., Daigger, G.T., Sandino, J., 2009. Modeling integrated fixed film activated sludge (IFAS) and moving biofilm reactor (MBBR) systems I: Mathematical treatment and model development. Water Environ. Res. 81, 555–575.

Calderón, K., Martín-Pascual, J., Poyatos, J.M., Rodelas, B., González-Martínez, A., González-López, J., 2012. Comparative analysis of the bacterial diversity in a lab-scale moving bed biofilm reactor (MBBR) applied to treat urban wastewater under different operational conditions. Bioresour. Technol. 121, 119–126.

Chu, L., Wang, J., 2011a. Comparison of polyurethane foam and biodegradable polymer as carriers in moving bed biofilm reactor for treating wastewater with a low C/N ratio. Chemosphere 83, 63–68.

Chu, L., Wang, J., 2011b. Nitrogen removal using biodegradable polymers as carbon source and biofilm carriers in a moving bed biofilm reactor. Chem. Eng. J. 170, 220–225.

Chu, L., Wang, J., Quan, F., Xing, X.-H., Tang, L., Zhang, C., 2014. Modification of polyurethane foam carriers and application in a moving bed biofilm reactor. Process Biochem. 49, 1979–1982.

Christensson, M., Welander, T., 2004. Treatment of municipal wastewater in a hybrid process using a new suspended carrier with large surface area. Water Sci. Technol. 49, 207–214.

Downing, L.S., Boltz, J.P., Dempsey, M.J., Hubbell, S., Kulick, F., 2013. Nitrification in biofilm reactors. In: Operation of Nutrient Removal Facilities. Water Environment Federation (WEF) Manual of Practice No. 37.

Dubois, M., Gilles, K.A., Hamilton, J.K., Rebers, P.A., Smith, F., 1956. Colorimetric method for determination of sugars and related substances. Anal. Chem. 28, 350–356.

Dvořák, L., Lederer, T., Jirků, V., Masák, J., Novák, L., 2014. Removal of aniline, cyanides and diphenylguanidine from industrial wastewater using a full-scale moving bed biofilm reactor. Process Biochem. 49, 102–109.

Ferrai, M., Guglielmi, G., Andreottola, G., 2010. Modelling respirometric tests for the assessment of kinetic and

stoichiometric parameters on MBBR biofilm for municipal wastewater treatment. Environ. Modell. Softw. 25, 626–632.

Figueroa, L.A., Silverstein, J., 1992. The effect of particulate organic matter on biofilm nitrification. Water Environ. Res. 64, 728–733.

Forrest, D., 2014. Tertiary Nitrifying Moving Bed Biofilm Reactor: A Study of Carrier and Loading Effects on Nitrifying Kinetics, Biologically Produced Solids and Microbial Community. University of Otawa, Canada, PhD Thesis.

Gerardi, M.H., 2003. The Microbiology of Anaerobic Digesters. John Wiley & Sons, New Jersey.

Head, M.A., Oleszkiewicz, J.A., 2005. Nitrifying bacteria addition into reactors operating near washout conditions for nitrification. J. Environ. Eng. Sci. 4, 257–264.

Henze, M., van Loosdrecht, M.C.M., Ekama, G.A., Brdjanovic, D., 2008. Wastewater treatment development. In: Henze, M., van Loosdrecht, M.C.M., Ekama, G.A., Brdjanovic, D. (Eds.), Principles, Modelling and Design. IWA Publishing, London.

Hoang, V., Delatolla, R., Abujamel, T., Mottawea, W., Gadbois, A., Laflamme, E., Stintzi, A., 2014. Nitrifying moving bed biofilm reactor (MBBR) biofilm and biofilm response to long term exposure to 1 °C. Water Res. 49, 215–224.

Hu, B., Wheatley, A., Ishtchenko, V., Huddersman, K., 2011. The effect of shock loads on SAF bioreactors for sewage treatment works. Chem. Eng. J. 166, 73–80.

Javid, A.H., Hassani, A.H., Ghanbari, B., Yaghmaeian, K., 2013. Feasibility of utilizing moving bed biofilm reactor to upgrade and retrofit municipal wastewater treatment plants. Int. J. Environ. Res. 7, 963–972.

Kwok, W.K., Picioreanu, C., Ong, S.L., van Loosdrecht, M.C., Ng, W.J., Heijnen, J.J., 1998. Influence of biomass production and detachment forces on biofilm structures in a biofilm airlift suspension reactor. Biotechnol. Bioeng. 58, 400–407.

Lewandowski, Z., Beyenal, H., 2014. Fundamentals of Biofilm Research, second ed. CRC Press, Boca Raton, FL, USA.

Melin, E., Helness, H., Kenakkala, T., Ødegaard, H., 2004. High-rate wastewater treatment based on moving bed biofilm reactor, polymer coagulation and flotation. In: Hahn, H.H., Hoffmann, E., Ødegaard, H. (Eds.), Chemical Water and Wastewater Treatment VIII. IWA Publishing, London.

Melin, E., Leiknes, T., Helness, H., Rasmussen, V., Ødegaard, H., 2005. Effect of organic loading rate on a wastewater treatment process combining moving bed biofilm and membrane reactors. Water Sci. Technol. 51, 421–430.

Mašic, A., Eberl, H.J., 2014. A modelling and simulation study of the role of suspended microbial populations in nitrification in a biofilm reactor. Bull. Math. Biol. 76, 27–58.

Matsumoto, S., Terada, A., Tsuneda, S., 2007. Modeling of membrane-aerated biofilm: effects of C/N ratio, biofilm thickness and surface loading of oxygen on feasibility of simultaneous nitrification and denitrification. Biochem. Eng. J. 37, 98–107.

Metcalf & Eddy, 2003. Wastewater Engineering: Treatment and Reuse, fourth ed. McGraw Hill, New York, NY.

Nof, K., Assulin, N., Galer, Y., Carreón, R.C.G., 2013. Improving particles separation after moving bed biofilm reactor (MBBR) systems by media clarifier. In: Proceeding of the 86th Annual Water Environment Federation Technical Exhibition and Conference, Chicago, IL, USA.

Ødegaard, H., 2006. Innovation in wastewater treatment: the moving bed biofilm process. Water Sci. Technol. 53, 17–33.

Ødegaard, H., Cimbritz, M., Christensson, M., Dahl, C.P., 2010. Separation of biomass from moving bed biofilm reactors (MBBRs). Proc. Water Environ. Fed. 22, 212–233.

Ødegaard, H., Gisvold, B., Strickland, J., 2000. The influence of carrier size and shape in the moving bed biofilm process. Water Sci. Technol. 41, 383–391.

Ohashi, A., de Silva, D.G.V., Mobarry, B., Manem, J.A., Stahl, D.A., Rittmann, B.E., 1995. Influence of substrate C/N ratio on the structure of multispecies biofilms consisting of nitrifiers and heterotrophs. Water Sci. Technol. 32, 75–84.

Piculell, M., Welander, T., Jönsson, K., 2014. Organic removal activity in biofilm and suspended biomass fractions of MBBR systems. Water Sci. Technol. 69, 55–61.

Randall, C.W., Pattarkine, V.M., McClintock, S.A., 1992. Nitrification kinetics in single-sludge biological nutrient removal activated sludge systems. Water Sci. Technol. 25, 195–214.

Rittmann, B.E., Manem, J.A., 1992. Development and experimental evaluation of a steady-state, multispecies biofilm model. Biotechnol. Bioeng. 39, 914–922.

Rusten, B., McCoy, M., Proctor, R., Siljudalen, J.G., 1998. The innovative moving bed biofilm reactor/solids contact reaeration process for secondary treatment of municipal wastewater. Water Environ. Res. 70, 1083–1089.

van Haandel, A.C., van der Lubbe, J.G.M., 2012. Handbook of Biological Wastewater Treatment. Design and Optimisation of Activated Sludge Systems, second ed. IWA Publishing, London, pp. p816.

Wang, J.L., Wu, L.B., 2004. Wastewater treatment in a hybrid biological reactor (HBR): nitrification characteristics. Biomed. Environ. Sci. 17, 373–379.

Zhang, T.C., Bishop, P.L., 1994. Density, porosity and pore structure of biofilms. Water Res. 28, 2267–2277.

Supplementary Material

Effect of increasing organic loading rates on the performance of moving-bed biofilm reactors filled with different support media: assessing the activity of suspended and attached biomass fractions

J. P. Bassin*, I. N. Dias, S. M. S. Cao, E. Senra, Y. Laranjeira, M. Dezotti

Federal University of Rio de Janeiro, COPPE - Chemical Engineering Program, Rio de Janeiro, Brazil

* Corresponding author. Mailing address: Chemical Engineering Program/COPPE, Federal University of Rio de Janeiro, P.O. Box 68502, 21941-972, Rio de Janeiro, Brazil. Tel. +55 21 25628347, Fax +55 21 25628300, Email address: jbassin@peq.coppe.ufrj.br

Kaldnes K1	Mutag Biochip

Figure S1: Illustration of the two different MBBR media (with no biomass attached) used in this study.

Table S1: Characteristics of the support media used in this study (information provided by Kaldnes and Mutag Umwelttechnologie AG).

Characteristic	Carrier material	
	Kaldnes K1	**Mutag Biochip**
Material	High-density polyethylene	Virgin polyethylene with additives
Shape	Cylinder	Round/parabolic
Nominal diameter (mm)	9.1	22
Nominal length/thickness (mm)	7.2	0.8 – 1.2
Apparent density (kg/m^3)	150	170
Specific surface area (m^2/m^3)	500	3000
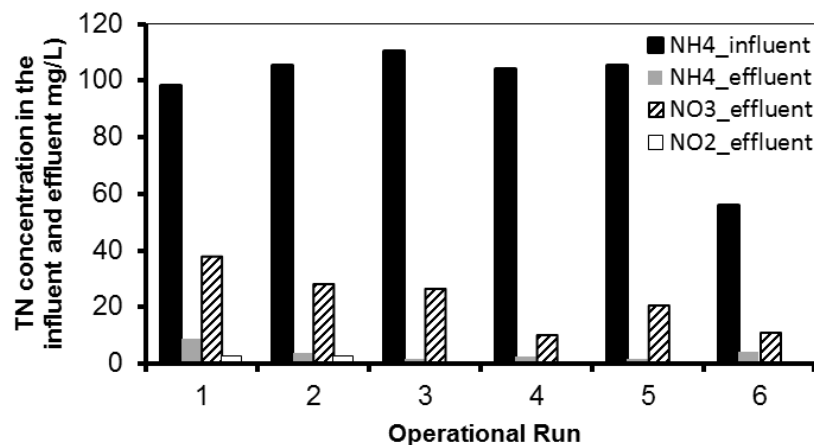
(a) MBBR₁
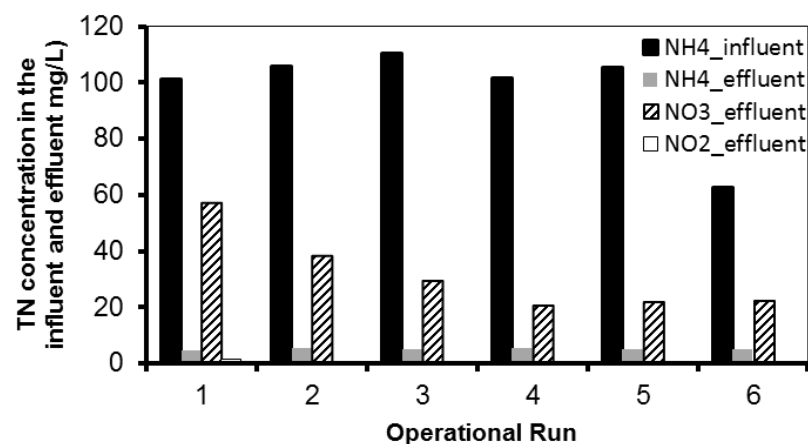
(b) MBBR₂

Figure S2: Total nitrogen concentrations in the influent (entirely as ammonium) and in the effluent (as remaining ammonium, nitrate and nitrate) of (a) MBBR₁ and (b) MBBR₂. Both reactors were subjected to the same influent ammonium concentration (black-filled bars) over the six experimental stages.
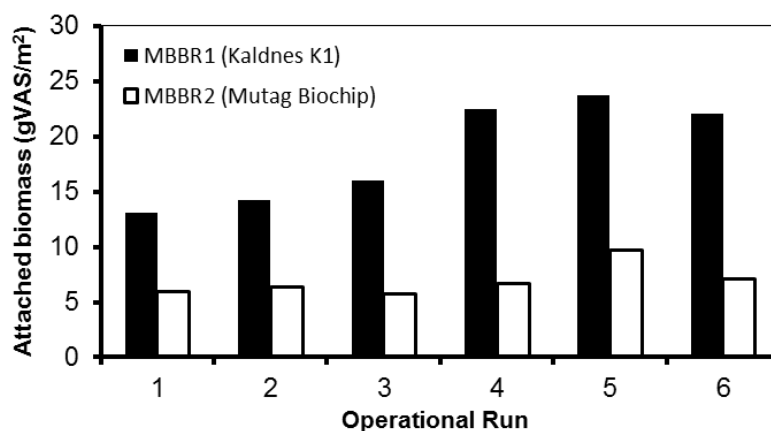

Figure S3: Surface biomass content in MBBR₁ and MBBR₂ over the six experimental runs. The amount of VAS per m² was calculated based on the total area for biofilm development in the reactor volume, which was chosen to be the same in both reactors (0.25 m²).
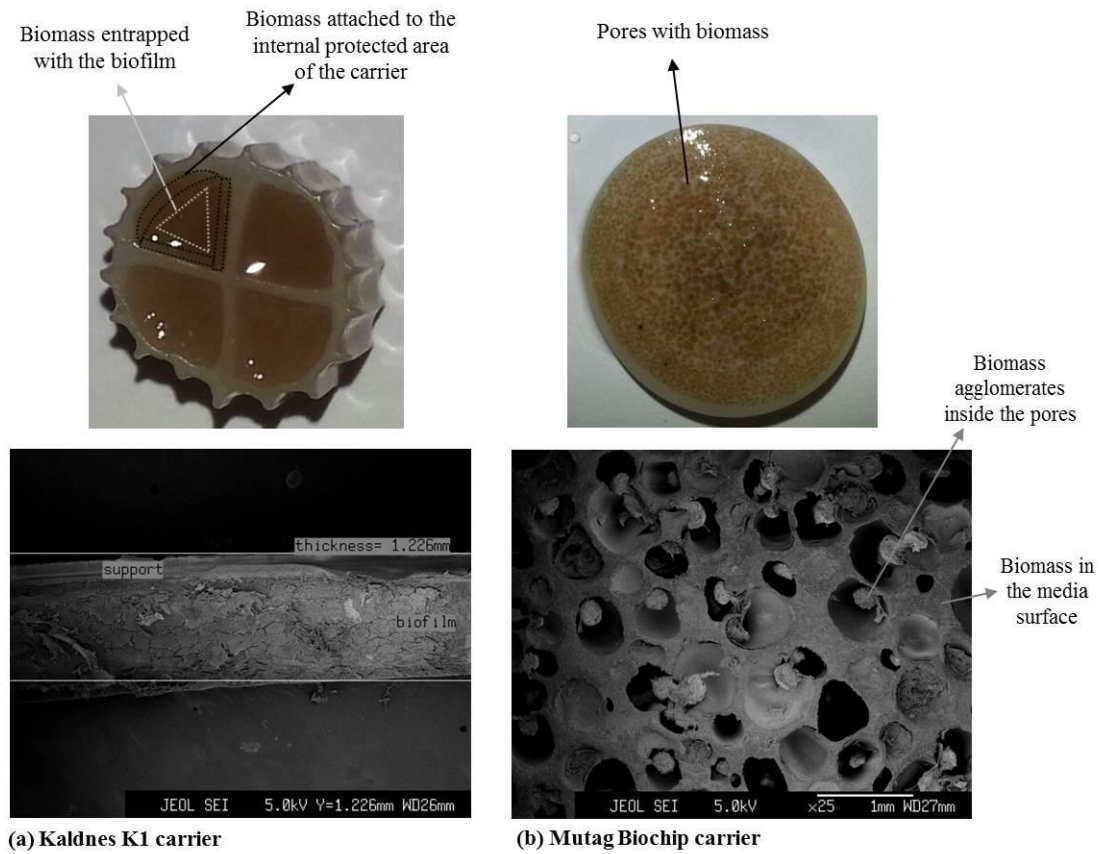
Figure S4: Illustration of the plastic carriers with attached biomass sampled in run 4, when the highest organic load applied was reached. Scanning electron microscopy (SEM) analysis was carried out to observe the biofilm conformation in both (a) Kaldnes K1 and (b) Mutag Biochip media. In (a) the magnification is indicated by the biofilm thickness measurement, whereas in (b) it was 25x, as displayed in the bottom part of the SEM image.
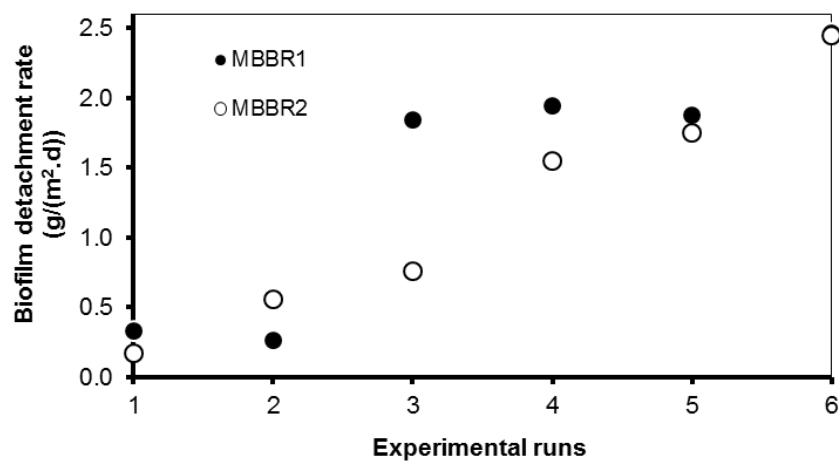
Figure S5: Average biofilm surface specific detachment rate (k_d) determined for the six experimental conditions applied to each MBBR.
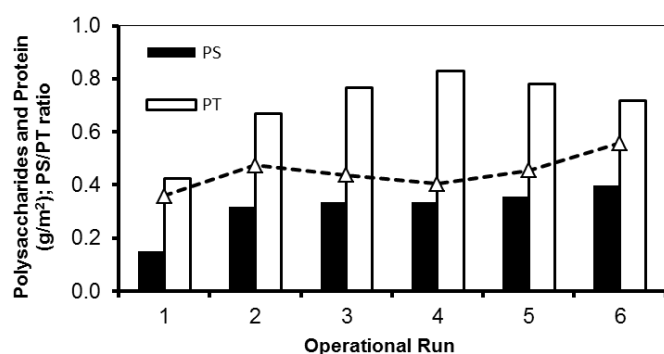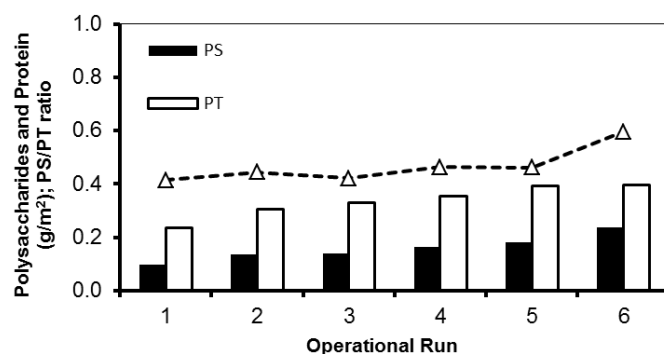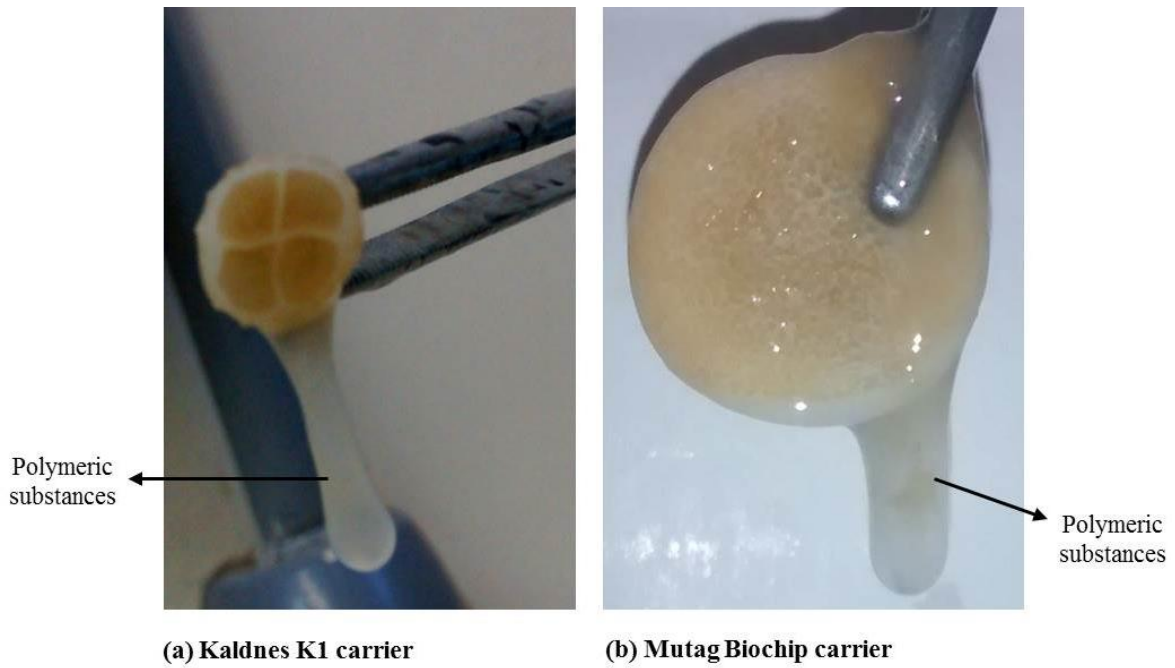
(a) MBBR$_1$ (b) MBBR$_2$

Figure S6: Total polysaccharides (PS) and protein (PT) contents of the attached biomass in MBBR$_1$ (a) and MBBR$_2$ (b). The results for both PS and PT are expressed in g/m^2 of support. The ratio between PS and PT is also plotted and indicated by the dashed line.

(a) Kaldnes K1 carrier   (b) Mutag Biochip carrier

Figure S7: Illustration showing the overproduction of gelatinous polymeric substances by the attached biomass in run 6.
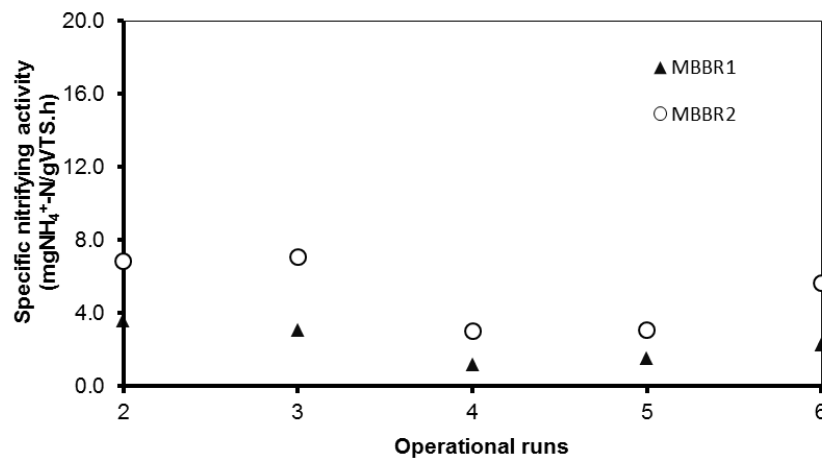
Figure S8: Ammonium removal rate per amount of biomass (VAS +VSS = VTS) from runs 2 to 6. For better comparison, the y-axis range used here in the same as that displayed in Figure 6, where the VAS- and VSS-specific nitrifying activities are shown. The activity batch test was not carried out in run 1.

Table S2: Volumetric ammonium removal rates obtained with either attached or suspended biomass from runs 2 – 6.

Experimental run	MBBR$_1$ Volumetric ammonium removal rate (mgNH$_4$-N/(L.h))[a]		MBBR$_2$ Volumetric ammonium removal rate (mgNH$_4$-N/(L.h))[a]	
	Suspended biomass	Attached biomass	Suspended biomass	Attached biomass
2	8.20	7.40	7.23	6.34
3	12.40	3.88	11.10	3.70
4	9.23	1.23	8.59	1.16
5	7.30	3.12	8.58	2.44
6	4.90	9.15	6.02	8.30

[a] The contribution of each type of biomass (attached or suspended) to the overall ammonium removal was estimated based on the volumetric ammonium removal rate obtained with the corresponding biomass fraction.

Calculation of biofilm surface specific detachment rate (k_d)

Biofilm surface specific detachment rate (k_d), expressed as $\left[\dfrac{gVSS}{m^2 \cdot d} \right]$, was calculated at the steady state condition of each experimental run, according to Equation (S1).

$$k_d = \frac{r_x}{A_{total\_biofilm}} \qquad\qquad (S1)$$

Where r_x is the total solids (TS=TAS+TSS) production rate, calculated according to Equation (S2) and expressed as $\left[\dfrac{gTS}{d} \right]$; and $A_{total\_biofilm}$ is the total surface area of the carrier available for biofilm growth, calculated by means of Equation (S3).

$$r_x = Q_{effluent} \cdot X_i \qquad\qquad (S2)$$

Where $Q_{effluent}[L/d]$ is the reactor effluent flow, $X_i[gTSS/L]$ is the concentration of biomass in the effluent of the corresponding reactor at the steady state condition of each experimental run;

$$A_{total\_biofilm} = A_{biofilm} \cdot V_{reactor} \cdot (V_S/V_R) \qquad\qquad (S3)$$

Where $A_{biofilm}$ is the specific surface area of each carrier available for biomass deposition ($A_{biofilm}$ = 500 m^2/m^3 for Kaldnes K1 (MBBR$_1$) and $A_{biofilm}$ = 3000 m^2/m^3 for Mutag Biochip (MBBR$_2$)), $V_{reactor}$ is the volume of the reactors (0.001 m^3); and (V_S/V_R) is the media filling ratio of each system ((V_S/V_R) = 0.5 in MBBR$_1$ and (V_S/V_R) = 0.083 in MBBR$_2$). The $A_{total\_biofilm}$ was therefore 0.25 m^2 for both reactors.